Z. Kristallogr. Suppl. **26** (2007) 495-501

Modulation of Cu-O chain length in $SmBa_2Cu_3O_{6+\delta}$, by Al doping and clustering

M. Scavini[1], M. Daldosso[1], M. Brunelli[2,*], C. Ferrero[2], C. Oliva[1]

[1]Dipartimento di Chimica Fisica ed Elettrochimica dell'Università di Milano, I-20133 Milano, Italy
[2]European Synchrotron Radiation Facility, av. J. Horowitz, BP 220, 38043 Grenoble Cedex, France

[*] Contact author; e-mail: brunelli@esrf.fr.

Keywords: synchrotron X-ray powder diffraction, pair distribution function analysis, cuprate superconductors, doping

Abstract. Inhomogeneity and disorder are crucial in determining the physical properties of nanostructured systems in which several physical interactions are active among strongly correlated components. The specific role of short range Cu-O chain ordering on the raising of superconductivity in $SmBa_2Cu_3O_{6+\delta}$ superconductors is discussed in this work. We have examined two Al-doped $SmBa_2Cu_3O_{6+\delta}$ samples having equal aluminium and oxygen concentration but different mean Cu-O chain lengths. The long and short range structures of the two samples have been determined through the parallel real space and Q space analysis.

Introduction

The physical properties of strongly correlated systems depend on structural disorder [1] at short (distortion around a point defect), middle (clustering of defects) and long range in a complex manner. This is the case, for instance, of $REBa_2Cu_3O_{6+\delta}$ (RE = Y, Ln; $0 \le \delta \le 1$) superconductors (SC), which are antiferromagnetic charge-transfer insulators for $\delta \approx 0$, but show metallic-like conduction and undergo a superconductive transition at $T_C \approx 90$ K for $\delta \approx 1$ [2]. RE = Sm is a member of this family of SC. The structure of $SmBa_2Cu_3O_6$ is described in [3]. For $\delta = 1$, $SmBa_2Cu_3O_7$ is orthorhombic (space group *Pmmm*). As a consequence of the removal of the fourfold axis, O2 at (½, 0, z) and O3 at (0, ½, z) are no longer equivalent as well as O4 at (0, ½, 0) and O5 at (½, 0, 0); the O4 site is nearly fully occupied while the O5 site is nearly empty [4].
In the literature, there is a general agreement on the close relation between the above structural changes and the increase of the hole concentration in the superconducting Cu2-O2/O3

planes [5]. This, in turn, is due to charge transfer (CT) from the Cu1-O4 chains, where oxidation occurs, to the Cu2-O2/3 planes. Clarification of the actual driving force for CT is highly desirable both for the full comprehension of the physical properties of this class of materials and for the design of new superconductors. The main obstacle to this purpose is that, while increasing δ, divers concomitant structural changes occur [6], thus it is necessary to separate individual structural effects, by producing samples with only one significant structural difference. This is obtained, for instance, through suitable doping. In Al-doped $SmBa_2Cu_3O_{6+\delta}$, Al substitutes Cu only in the Cu1 (0, 0, 0) position, occupying one of the four non equivalent (x, x, 0), x = ±0.06 sites [3,7]. Its role is to cut the Cu1-O4 chains in oxidised samples into fragments whose mean length is a function of the Al concentration and distribution. In a recent work [8] it has been evidenced the enhancement of the superconducting properties (T_c and Meissner fraction) of $SmBa_2Cu_{3-x}Al_xO_{6+\delta}$ samples where Al clustering was induced throughout a suitable annealing route [9], in respect to non-clusterised samples with the same Al concentration and oxygen non-stoichiometry δ (i.e. with the same total hole concentration [10]). In this paper, it will be shown that the process of Al clustering produces samples with different mean Cu1-O4 chain lengths. This has been revealed by joint Rietveld and PDF analysis using synchrotron X-ray powder diffraction data.

Experimental

Polycrystalline samples of $SmBa_2Cu_{2.85}Al_{0.15}O_{6+\delta}$ were synthesised by solid state reaction starting from BaO_2 (Aldrich 95%), Sm_2O_3, CuO and Al_2O_3 (all Aldrich 99.99%). Powders were mixed, pressed into pellets, and allowed to react in pure oxygen at 960°C for a total time of 96 hours with one intermediate cooling, grinding and repelletisation step. The as-prepared samples were annealed for 96 hours at T = 400°C and $P(O_2)$ = 1 atm in quartz ampoules and then quenched to room temperature to induce oxidation ("sample A"). Aluminum clusterisation ("sample B") has been obtained by following the procedure suggested by Brecht [9]: an aliquot of the as prepared sample has been annealed at T = 800°C and $P(O_2) = 10^{-4}$ atm for 96 hours and at 400°C and $P(O_2)$ = 1 atm for the same amount of time.
Synchrotron X-ray powder diffraction (XRPD) patterns were collected at the high-resolution powder diffraction beam line ID31 at ESRF, Grenoble, France [11]. Samples were loaded in 0.6 mm diameter glass capillary, mounted on the axis of the diffractometer and spun during measurements; the samples were cooled to 80 K. Powder diffraction patterns were collected with a maximum value of the wave vector $Q_{max} = 18.7$ Å^{-1} at a wavelength of 0.33483(1) Å. Data were recorded for longer times at higher angles in order to increase statistical significance and for extraction of good quality PDF with reduced noise at high Q [12]. Rietveld refinement on the experimental patterns has been performed using the GSAS software suite [13] and its graphical interface EXPGUI [14], while for real space analysis the programs PDFGetX [15] and PDFFIT [16] have been used.

Results

Rietveld analysis on sample A was carried out describing the system in a tetragonal cell (space group *P*4/*mmm*). Cell parameters, atomic positions, isotropic thermal factors and occupancies were refined; atomic positions from the literature were used as a starting point

[7]. First attempts to refine the structural model of sample B gave very poor results. Only with a system composed of an Al-rich tetragonal phase and an Al-poor orthorhombic phase could the experimental data be interpreted in a satisfactory way (see figure 1b). The XRPD pattern of sample B has been interpreted using two structural models: in model 1 all the positional and thermal parameters are supposed to be identical for the two phases while in model 2 the positional coordinates and the Al concentration have been varied independently. In model 2 the Al concentration increases in the tetragonal phase with respect to the orthorhombic phase (see Table 1), so as to enforce the idea that Al clustering is the driving force of the phase separation observed with sample B. Final Rietveld refinement (figure 2) converged to $R_{wp} = 8.9\%$ and $\chi^2 = 2.6$.

Rietveld analysis has revealed the presence of an orthorhombic phase in sample B. This implies the presence of Cu1-O4 chains fragments of non-negligible length. In order to determine the length of these chain fragments, the same data have been analysed in the real space using PDF analysis. The corresponding G(r) patterns in real space for sample A and for sample B are plotted in figure 3a: the two are largely overlapping in the given r interval, within the given data resolution. However, differences arise at higher r values; at the same time the amplitudes of the G(r) oscillations decrease more rapidly with B than with A sample with increasing r (see figure 3b). A similar decrease of PDF peak heights as a function of r has been noted by Kim and co-workers [17] and used to show the nanoscaled domain structure of β-Zn_4Sb_3. In order to quantify the last experimental evidence we interpreted both data sets employing simple monophasic primitive-cell models. Refinements have been performed on both samples in the $3 < r < 20$ Å range varying atomic positions and isotropic thermal parameters (figure 4a). Further refinements have been performed using small intervals of the G(r) curves and varying solely scale factors and cell parameters. sf_A and sf_B are the overall scale factors for the G(r) of samples A and B, respectively. A gradual decrease of the sf_B/sf_A ratio *vs*. r is apparent for $r > 20$ Å (figure 4b). Since the data for the two samples have been collected under identical experimental conditions and identical corrections have been made, this behaviour can be safely ascribed to a decrease of local order within sample B as compared to sample A for interatomic distances larger than 20 Å. In other words, for $r > 20$ Å, interatomic vectors within ordered regions become less frequent than inter-domain ones, which causes a progressive decrease of the G(r) oscillations in sample B. Since disorder is introduced in the structure by Al doping which causes displacement of neighbouring ions (mainly O1 and Ba ions [18]), the value of 20 Å should correspond to the average width of orthorhombic Al-free domains and then to the average length of Cu1-O4 chain fragments within the sample B.

Conclusion

In this work, we have reported the combined real and reciprocal space analysis of XRPD patterns measured on two $SmBa_2Cu_{2.85}Al_{0.15}O_{6+\delta}$ samples produced with identical Al concentrations and very close O contents (*i.e.* same total hole concentration), giving rise to similar structures but different Al distribution (namely, sample A and B). In sample A the Al ions were randomly distributed, while in sample B Al clustering was induced throughout a suitable annealing route. The X-ray diffraction pattern corresponding to sample A was interpreted using a single tetragonal phase, while a biphasic model composed of an Al-rich

tetragonal phase and an Al-poor orthorhombic phase was necessary to interpret in a satisfactory way the X-ray diffraction pattern of sample B, thus revealing longer mean Cu1-O4 chain lengths in Al-poor orthorhombic domains. Furthermore, by applying local structure PDF analysis, we were able to estimate the length of such chain fragments within sample B to be ~ 20 Å, confirming − as previously shown [8] − that Cu1-O4 ordering at nanometric scale plays a significant role in inducing superconductivity in $REBa_2Cu_3O_{6+\delta}$ compounds.

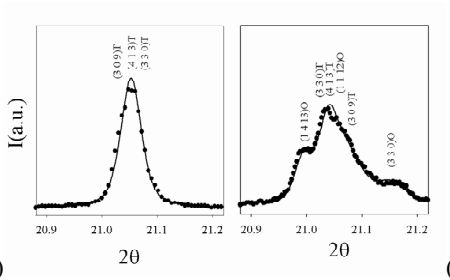

Figure 1. a) Details of the experimental (circles) and of the calculated (full lines) XRPD patterns relative to sample A and b) to sample B. O and T beside the Miller indices refer to the orthorhombic and tetragonal phases, respectively. The results of the refinements are reported in Table 1.

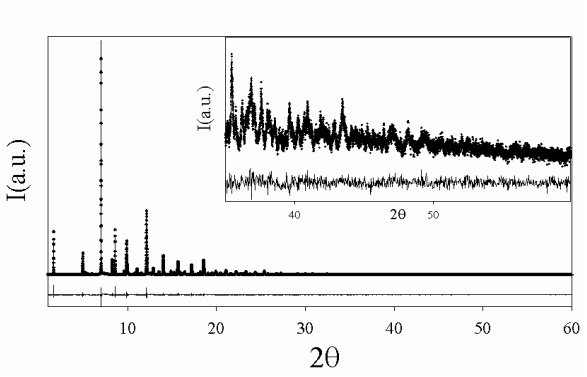

Figure 2. Observed (crosses), calculated (continuous line) and difference plot (bottom) of the final Rietveld refinement of the structural model for the clusterised sample B. The inset highlights the good quality of the data in the high angle range of the powder diffraction pattern.

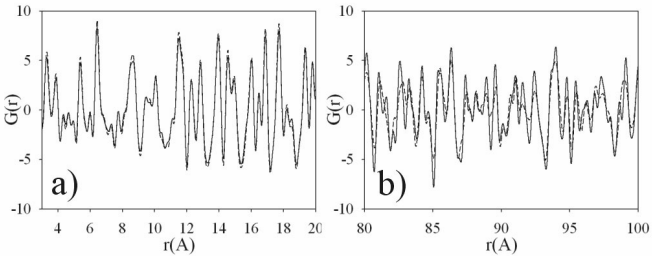

Figure 3. Comparison of the pair distribution function G(r) for sample A (continuous line) and for sample B (dashed line) at low-r (a) and high-r (b) values.

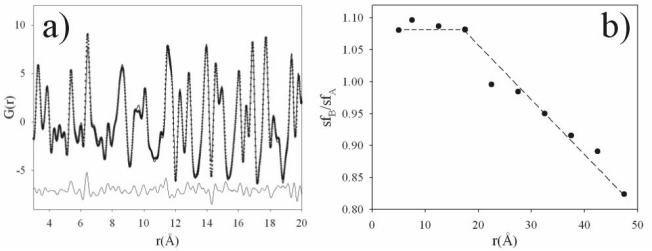

Figure 4. – a) Experimental (circles), calculated (black line) and residuals (bottom) G(r) refinement of an orthorhombic cell model for sample B in the 3 < r < 20 Å range (R_{wp} = 12.2%). b) sf_A/sf_B ratio (circles) as a function of r. The lines are guides for the eyes.

Table 1. Structural parameters and agreement factors for samples A and B as determined from X-ray diffraction data. Isotropic thermal parameters (U_{iso}: Å^2), atomic z coordinate (z) and occupation factors (of: atoms/cell). Bolds characters correspond to not-refined parameters.

	Sample A	Sample B model 1		Sample B model 2	
		Phase 1	Phase 2	Phase 1	Phase 2
Space group	*P4/mmm*	*P4/mmm*	*Pmmm*	*P4/mmm*	*Pmmm*
Weight Frac-	1	0.444(3)	0.557(2)	0.466(3)	0.534(3)
a/Å	3.88826(2)	3.89091(3)	3.86702(6)	3.89099(3)	3.86686(6)
b/Å	≡a	≡a	3.90140(4)	≡a	3.90142(4)
c/Å	11.6651(1)	11.6418(2)	11.6741(1)	11.6415(2)	11.6742(1)
Uiso(Sm)	0.0020(1)	0.0015(1)	≡ phase 1	0.0014(1)	≡ phase 1
zBa	0.18500(8)	0.18370(5)	≡ phase 1	0.1829(1)	0.1845(1)
Uiso(Ba)	0.0063(2)	0.0058(1)	≡ phase 1	0.0058(1)	≡ phase 1
Uiso (Cu1/Al1)	0.0090(4)	0.0061(3)	≡ phase 1	0.0059(3)	≡ phase 1
zCu2	0.3531(1)	0.35300(9)	≡ phase 1	0.3529(2)	0.3529(2)
Uiso(Cu2)	0.0026(2)	0.0020(2)	≡ phase 1	0.0020(2)	≡ phase 1
zO1	0.157(1)	0.1562(6)	≡ phase 1	0.155(1)	0.157(1)
Uiso(O1)	0.009(1)	0.006(1)	≡ phase 1	0.008(1)	≡ phase 1
zO2/O3	0.3731(5)	0.3748(3)	≡ phase 1	0.3705(7)	0.3782(6)
Uiso(O2/O3)	0.0051(9)	0.0060(8)	≡ phase 1	0.0060(8)	≡ phase 1
Uiso(O4/O5)	0.012(4)	0.022(3)	≡ phase 1	0.010(2)	≡ phase 1
o.f.(Cu1)	**0.85**	**0.85**	**0.85**	0.808(9)	0.892(9)
o.f.(Al1)	**0.15**	**0.15**	**0.15**	0.192(8)	0.108(8)
o.f.(O4)	**0.98**	**0.96**	**0.96**	**0.96**	0.69(2)
o.f.(O5)	**---**	**---**	**0.00**	**---**	0.27(2)
Rp	0.085	0.073		0.069	
Rwp	0.105	0.093		0.089	

References

1. Dagotto, E., 2005, *Science*, **309**, 257.
2. Skakle, M.S., 1998, *Mater. Sci. Eng.*, **R23**, 1 and references therein.
3. Scavini, M.& Bianchi, R., 2001, *J. Sol. State. Chem.*, **161**, 396.
4. Guillaume, M., Allenspach, P., Henggeler, W., Mesot, J., Roessli, B., Staub, U., Fischer, P., Furrer A. & Trounov, V., 1994, *J. Phys.: Condens. Matter*, **6**, 7963.
5. Tolentino, H., Baudelet, F., Fontaine, A., Gourieux, T., Krill, G., Henry, J.Y., & Rossat Mignod, J.,1992, *Physica*, **C192**, 115.
6. Andersen, N. H. *et al.*, 1999, *Physica*, **C317-318**, 259.
7. Dupree, R., Gencten, A. & Paul, D.McK., 1992, *Physica*, **C193**, 81.
8. Scavini, M., Daldosso, M., Cappelli, S., Oliva, C., Brunelli, M., Ferrero, C., Lascialfari, A., 2006, *Europhys. Lett.*, **76**, 443
9. Brecht, E., Schmahl, W.W., Miehe, G., Rodewald, M., Fuess, H., Andersen, N.H., Hanssmann, J. & Wolf, Th., 1996, *Physica*, **C265**, 53.

10. Scavini, M., Mollica, L. & Malavasi, L., 2004, *Sol. Stat. Sci.*, **6**, 1187.
11. Fitch, A. N., 2004, *J. Res. Natl. Inst. Stand. Technol.*, **109**, 133.
12. Brühne S., Eckhard Uhrig, I., Luther, K.-D., Assmus, W., Brunelli, M., Masadeh, A.S. & Billinge S.J.L., 2005, *Z. Kristallogr.*, **220** 962–967.
13. Larson, A.C. & Von Dreele, R.B., 1994, *GSAS: General Structural Analysis System* (Los Alamos National Laboratory: Los Alamos, NM).
14. Toby, B. H., 2001, *J. Appl. Cryst.*, **34**, 210.
15. Jeong, I.K., Thompson, J., Proffen, Th., Turner A.M.P. & Billinge, S.J.L., 2001, *J. Appl. Cryst.*, **34**, 536.
16. Proffen, Th. & Billinge, S.J.L., 1999, *J. Appl. Cryst.*, **32**, 572.
17. Kim, H. J., Bozin, E. S., Haile, S. M., Snyder, G. J., Billinge, S. J. L., 2006, *American Physical Society*, APS March Meeting, March 13-17, 2006, p. 16006
18. Daldosso M., 2004, *Studio del disordine a corto e medio raggio nell'ossido superconduttore* $SmBa_2Cu_{3-x}Al_xO_{6+\delta}$ *in funzione del drogaggio* (Master thesis, Milano, Italy)

Acknowledgements. The authors acknowledge the European Synchrotron Radiation Facility for provision of synchrotron radiation time; they also wish to thank Dr. A. N. Fitch for assistance in using beam line ID31 and Prof. Simon J.L. Billinge for useful discussions.